

# Crystalline ethane-1,2-diol does not have intra-molecular hydrogen bonding: Experimental and theoretical charge density studies

Deepak Chopra<sup>a,c</sup>, Tayur N. Guru Row<sup>a,\*</sup>, Elangannan Arunan<sup>b</sup>, Roger A. Klein<sup>d</sup>

<sup>a</sup> Solid State and Structural Chemistry Unit, Indian Institute of Science, Bangalore 560 012, India

<sup>b</sup> Department of Inorganic and Physical Chemistry, Indian Institute of Science, Bangalore 560 012, India

<sup>c</sup> Department of Chemistry, Indian Institute of Science Education and Research, ITI (Gas Rahat Building), Bhopal 462 023, India

<sup>d</sup> Institute for Physiological Chemistry, University of Bonn, D-53115 Bonn-Poppelsdorf, Germany

## ARTICLE INFO

### Article history:

Received 9 October 2009

Received in revised form 4 November 2009

Accepted 9 November 2009

Available online 15 November 2009

### Keywords:

*In situ* cryocrystallization

Experimental charge density

Conformation analysis

Inter-molecular interactions

*Ab initio* calculations

## ABSTRACT

The X-ray structure and electron density distribution of ethane-1,2-diol (ethylene glycol), obtained at a resolution extending to  $1.00 \text{ \AA}^{-1}$  in  $\sin \theta/\lambda$  (data completion = 100% at 100 K) by *in situ* cryocrystallization technique is reported. The diol is in the *gauche* (*g'Gt*) conformation with the crystal structure stabilised by a network of inter-molecular hydrogen bonds. In addition to the well-recognized O–H...O hydrogen bonds there is topological evidence for C–H...O inter-molecular interactions. There is no experimental electron density based topological evidence for the occurrence of an intra-molecular hydrogen bond. The O...H spacing is  $\sim 0.45 \text{ \AA}$  greater than in the gas-phase with an O–H...O angle close to  $90^\circ$ , calling into question the general assumption that the *gauche* conformation of ethane-1,2-diol is stabilised by the intra-molecular oxygen–hydrogen interaction.

© 2009 Elsevier B.V. All rights reserved.

## 1. Introduction

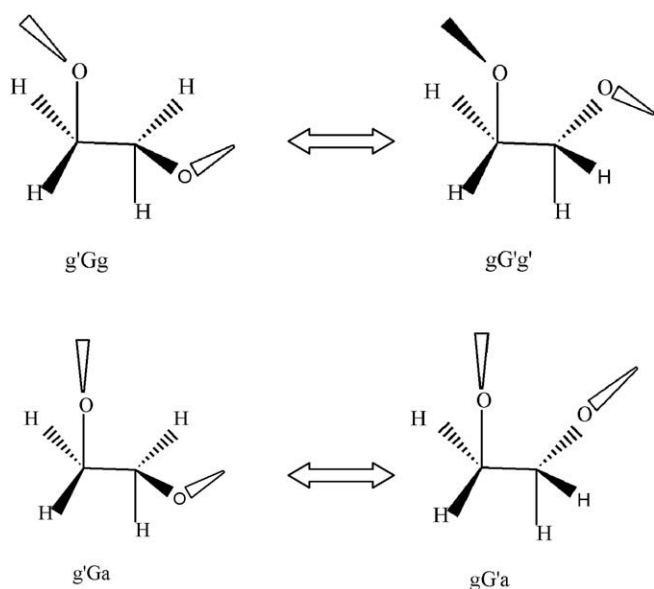
Intra-molecular hydrogen bonding in ethane-1,2-diol is one of the many unicorns of chemistry in the sense meant by Frenking and Krapp (2007), representing "...a mystical animal whose appearance is known to everybody although nobody has ever seen one..." [1]. It has commonly been taken for granted as the reason for ethane-1,2-diol assuming the *gauche* conformation in the gas-phase and for the red-shift in the O–H vibrational stretching frequency [2], although recent theoretical studies have called this assumption into question [3]. Its existence continues to be asserted, rather than proven, by statements such as the recent one by Lopes Jesus et al. (2006) "...It is well known [sic] that intra-molecular hydrogen bonding plays an important role in conformers of 1,2-ethanediol... [and, by extension, for other ( $n, n + 1$ )-diols]..." [4].

Electron diffraction measurements had demonstrated that the preferred conformation of free ethane-1,2-diol was characterised by the two C–O bonds being *gauche* with respect to one another (Scheme 1), with a dihedral angle O–C–C–O of around  $65^\circ$  [5]. Early infrared studies in gas, liquid and solid phases pointed to the predominance of the *gauche* form, claiming the gas-phase results as evidence for intra-molecular hydrogen bonding as the stabilising

force, discussed in detail in the next paragraph [6]. The microwave spectroscopy of ethane-1,2-diol has been extensively studied for nearly 35 years [7] and it is now well established that the most energetically favourable conformations at room temperature are the *g'Gt* (also known as *g'Ga*) and *g'Gg* rotamers, or their energetically equivalent mirror-images *gG't* (*gG'a*) and *gG'g'* (Scheme 1) [8,9]. Earlier, X-ray diffraction studies on ethane-1,2-diol indicated the presence of *trans* conformer [10a–c]. Recent X-ray diffraction studies on liquid ethane-1,2-diol have identified only the *gauche* conformer [10d] and based on the results from earlier microwave and *ab initio* studies the presence of an intra-molecular hydrogen bond was proposed. Database analysis by Brock also indicated the dominance of the *gauche* conformer for non-aromatic vicinal diols in the crystal structure [10e]. This analysis, however, did not show any unambiguous evidence for intra-molecular hydrogen bonding in any of the vicinal diols. The single crystal structure determination (spherical atom refinement) of ethane-1,2-diol has been performed initially by Boese and co-workers wherein it was observed that the molecule exists in synclinal conformation. It was further observed that the crystal structure is stabilised by a network of "inter-molecular" O–H...O interactions [10f,10g]. There was no mention of C–H...O interactions.

The experimental evidence for an intra-molecular O–H...O hydrogen bond in ethane-1,2-diol and that this stabilises the *gauche* conformation, relies heavily on the interpretation of a small red-shift in the vibrational stretching frequency for the 'bound'

\* Corresponding author. Tel.: +91 80 2293 2796; fax: +91 80 2360 1310.  
E-mail address: [ssctng@sscu.iisc.ernet.in](mailto:ssctng@sscu.iisc.ernet.in) (T.N. Guru Row).



**Scheme 1.** Experimentally favourable conformers of ethane-1,2-diol. ( $g'Gg$  and  $gG'g'$ ) and ( $g'Ga$  and  $gG'a$ ) pairs are mirror images of each other.

O–H group compared to the unbound O–H group [11–14]. The observed vapour-phase red-shift for ethane-1,2-diol is  $\sim 33\text{ cm}^{-1}$  [6] and in dilute carbon tetrachloride solution it is  $32\text{ cm}^{-1}$  [2]. In supercritical  $\text{CO}_2$  and Ar, the red-shift has been reported very recently as  $26\text{ cm}^{-1}$  and  $33\text{ cm}^{-1}$ , respectively, the difference being attributed to inter-molecular interaction with  $\text{CO}_2$  [11]. Recent theoretical anharmonic oscillator calculations at the QCISD/6-311++G(2d,2p) level of theory for the two most stable conformations ( $g'Gt$  and  $g'Gg$ ) [12a] give values of  $39\text{ cm}^{-1}$  and  $22\text{ cm}^{-1}$ , respectively, in excellent agreement with early experiments, although a previous paper from the same laboratory reports modern experimental measurements and theoretical calculations at the CCSD(T)/aug'-cc-pVTZ level giving relatively higher values but nonetheless in agreement with one another [12b]. Despite these small differences, it is clear that the red-shift is about  $30\text{ cm}^{-1}$  for the 'bonded OH' compared to the 'free OH'.

The crucial question, however, is whether the observation of a small red-shift constitutes *a priori* primary evidence of an interaction between the O–H...O atoms, or whether other effects may be responsible. The use of a red-shift for 'detecting' intra- and inter-molecular hydrogen bonding in diols and other molecules has a long historical pedigree [13]. Red-shifts for hydrogen bonded systems range from a few tens of wavenumbers to many hundreds of wavenumbers [14]. As has been pointed out recently, however, relatively small red-shifts of less than  $\sim 100\text{ cm}^{-1}$  can just as easily be caused by hyper-conjugative effects ( $[\text{C}-\text{H}] \Rightarrow [\text{O}-\text{H}]^*$  and  $[\text{O}-\text{H}] \Rightarrow [\text{C}-\text{H}]^*$ ) in the diol skeleton [3], more particularly in situations where there is no possibility of intra-molecular hydrogen bonding on geometric grounds. In particular, the O–H...O angle is  $100^\circ$ , which is below the generous limits of hydrogen bond angles recommended by Desiraju and Steiner [61]. Moreover, the 'non-bonded' O–H group in ethane-1,2-diol shows a red-shift on rotation from *trans* to *gauche*, i.e.,  $g'Gt \Rightarrow g'Gg$ , comparable in magnitude to the red-shift for the O–H...O interaction [3,11], explicable in terms of hyper-conjugative effects. Hence, it would be useful to have other experimental data for independent confirmation for example, NMR spin–spin coupling data [15] or changes in chemical reactivity or pK [16], and experimental electron density topology, which would make the diagnosis of intra-molecular hydrogen bonding more secure. Interestingly, recent NMR investigation of ethane-1,2-diol by Roberts and co-workers [17] led the

authors to conclude, that "the bulk of the NMR evidence indicates that intra-molecular hydrogen bonding between the hydroxyl groups is unlikely to be a significant factor in determining that preference, except possibly in fairly non-polar solvents. The 'gauche effect' is clearly very important, especially in aqueous solution". *Ab initio* and AIM theoretical studies have raised doubts about the existence of intra-molecular hydrogen bond, even in the case of monomer, as indicated earlier [3].

*Ab initio* and density functional theory (DFT) studies of the potential energy surface for ethane-1,2-diol show that the global minimum energy structure is the  $g'Gt$  conformer together with its mirror image  $gG't$ , followed by the  $g'Gg$  ( $gG'g'$ ) conformer a few tenths of a kcal/mol (0.3–0.4) less stable. The all-*trans* conformer  $tTt$  is  $\sim 2$ – $3$  kcal/mol less stable than the global minimum. The symmetric  $g'Gg'$  ( $gG'g$ ) conformer identified incorrectly by molecular mechanics as the global minimum is actually a first-order transition state [18], probably resulting from poor parametrization of the force-field for hydrogen bonding [19]. The two most stable conformers are similar for all 1,2-diols studied [20] and similar results have been obtained for propane-1,3-diol, butane-1,3-diol and butane-1,4-diol [21]. The theoretical calculations are all in keeping with the experimental observations.

The lack of a (3, –1) bond critical point (BCP) distinguishes all freely rotatable ( $n, n + 1$ )-diols and 2-substituted ethanols such as the 2-haloethanols or ethanolamine from, for example, propane-1,3-diol or butane-1,4-diol or, for that matter, any of the higher  $\alpha,\omega$ -diols, all of which possess a (3, –1) BCP [22,23]. These findings have been amply confirmed in the literature by a number of authors [24–26], although in one case the authors wished to claim that weak intra-molecular hydrogen bonding might still exist in spite of failing to satisfy their own self-imposed requirement that proton delocalisation be demonstrated [27]. Klein [22] has suggested, building on earlier work [28–29], that the presence or absence of a (3, –1) bond critical point is a useful marker of whether or not a hydrogen bond exists between a putative donor and acceptor. The presence of a BCP is central to the eight theoretical criteria listed by Koch and Popelier, though they have identified the mutual penetration of H and acceptor atom as the necessary and sufficient condition based on the examples covered in their work [28]. If the BCP is absent, the other seven parameters cannot be evaluated. Two of these parameters are the electron density and its Laplacian at the BCP, and these obviously cannot be determined. For establishing mutual penetration, the bonded radii are defined as the distances from the H and acceptor atom to the BCP. The distance from the donor/acceptor atom to the point at which the electron density of the monomer reduces to 0.001 a.u., along the hydrogen bond path is defined as the non-bonded radii. If the bonded radii for H and acceptor atoms are shorter than the corresponding non-bonded radii, there is mutual penetration. Clearly, this requires the presence of a BCP. The other four parameters are integrated properties of the H atom that is involved in H bonding and its boundary is defined by the BCP. Hence, all the eight criteria depend on the existence of a BCP. It also has the advantage, unlike many of the other parameters used to determine whether there is hydrogen bonding, that it is not continuous as is, for example, the red-shift which shows no abrupt change between bonding and no bonding [13,22]. Moreover, the bond critical point is experimentally accessible since the electron density distribution can be determined by X-ray or neutron diffraction using, for example, the Hansen–Coppens multipole expansion [30]. Though, mutual penetration of H and acceptor atoms as defined by Koch and Popelier is a quite reasonable criterion, in practice its calculation depends on the use of classical *van der Waals* radii as non-bonded radii, a concept that has been criticised in the context of hydrogen bonding [23,31–35]. The calculated atomic volume of the

donor hydrogen, out to the 0.001 a.u. contour, is very sensitive to hydrogen bonding and can show a reduction of ~70% for very strong interactions as a result of wave function contraction [31]. Weak interactions, however, produce correspondingly small changes in atomic volume, which are not particularly diagnostic.

The  $(n, n+m)$ -diols, including the  $\alpha,\omega$ -diols, all show a clear  $(3, -1)$  BCP well separated from its associated  $(3, +1)$  ring critical point (RCP) for values of  $m = 2-6$  [23], indicating intra-molecular O–H...O hydrogen bonding. IR red-shift, interaction energy, reduction in donor–acceptor distance, electron density at the BCP and the value of its Laplacian, all increase in the series propane-1,3-diol, butane-1,4-diol, pentane-1,5-diol and hexane-1,6-diol, peaking for the butane derivative which can be thought of as forming a highly stable six-membered ring with the intra-molecular hydrogen bond [23]. Recent work has suggested that the ability to form a  $(3, -1)$  BCP and hence an intra-molecular hydrogen bond in diols is associated with the orbital overlap integral for occupied–unoccupied (antibonding) interactions exceeding that for occupied–occupied (steric repulsion) interactions [36].

Interestingly,  $(n, n+1)$ -diols in highly strained ring systems such as the norbornanes in which the O–C–C–O dihedral is close to zero, also show a pronounced  $(3, -1)$  BCP for the O–H...O interaction [3]. On the other hand, the pendant O–H groups in 4C<sub>1</sub>-glucopyranose which have always been assumed to be cooperatively hydrogen bonded to one another [37], apart from having no  $(3, -1)$  BCP for the O–H...O interaction actually show the reverse effect, i.e., negative cooperativity [36].

The presence of a  $(3, -1)$  BCP is merely a mathematical topological consequence of the concentration of electron density around a line joining two nuclei, or a nucleus and a centre of electron density. The line need not necessarily be straight. This concentration of electron density around a line joining two interacting centres is what we commonly understand as the ‘chemical bond’. This should not be confused with the sign of the Laplacian at the BCP, which provides a measure of *relative* electron excess or deficiency, allowing the bond to be classified as either closed-shell or shared-shell [38]. It can be argued that in the absence of a bond critical point (BCP), it is difficult to maintain the position that there is bonding present. Lack of such a concentration of electron density between plausible hydrogen bond donor and acceptor atoms would mean that long-distance transmission of electron mediated effects such as embodied in the concept of the ‘electron wire’ [39], or the phenomena of cooperative networks would not be possible as, for example, in liquid water.

In this paper, we report results from a high-resolution charge density study using X-ray data on crystalline ethane-1,2-diol in which the diol is in the *gauche* conformation, stabilised by an extensive network of inter-molecular hydrogen bonds. There is no experimental electron density topological evidence for intra-molecular hydrogen bonding. Since the *gauche* conformation is stable even in the solid state with an O–H...O interaction distance ~0.45 Å greater than in the gas-phase, resulting in a greatly reduced O...H interaction energy, and in the clear absence of any intra-molecular hydrogen bonding, one must conclude that the primary driving force for the *gauche* effect in ethane-1,2-diol is not the oxygen–hydrogen interaction as formerly supposed. Whether or not ethane-1,2-diol forms an intra-molecular hydrogen bond has considerable significance since this molecule has been used as part of the training set for parametrising molecular mechanics programs [18] as well as being a ubiquitous synthon in sugars [40] and many pharmacologically active materials [41]. It is a monomer commonly used in step-growth polymerizations for the synthesis of polyesters and polyurethanes [42]. Clear understanding of the monomer properties is essential before one can model the bulk behavior using molecular mechanics programs.

## 2. Experimental

### 2.1. Sample preparation and data collection

A Lindemann glass capillary of ~2.5 cm length and 0.3 mm diameter was filled with the liquid, flame-sealed at one end and mounted on a Bruker AXS X-ray diffractometer equipped with a SMART APEX CCD area detector using Mo K $\alpha$  radiation (50 kV, 40 mA). On cooling very slowly at 30 K/h using an OXFORD Nitrogen cryo-system, complete solidification of the liquid in the capillary took place at 260 K. In the first attempt at this cooling rate, sample crystallinity was ensured by crossing over the glass transition in order to avoid possible glass formation. In order to obtain a single crystal inside the capillary, a temperature gradient was created by moving the nitrogen stream away from the goniometer initially and on subsequent melting of the solid, realigning the stream after a time delay. This process of annealing was repeated manually until a well-defined single crystal was obtained. A rotation photograph was taken at this stage to ascertain the quality of the diffraction spots. During data collection the temperature was maintained at  $100 \pm 2$  K with an Oxford Cryostream N<sub>2</sub> open-flow cryostat. Initially, 180 frames of data were collected with  $2\theta$  fixed at  $-25^\circ$ , exposure time of 10 s and a  $\omega$  scan width of  $-1^\circ$ . The frames obtained were then processed using SMART [43,44] software to determine the unit cell dimensions. The crystal structure was solved using SIR92 [45] and refined in SHELXL97 [46]. The geometric calculations were done using PARST [47] and PLATON [48]. All the hydrogen atoms were located from a Fourier difference map and refined isotropically.

The diffraction data were collected using SMART in three batches as detailed in Table S1, keeping the crystal-to-detector distance fixed at 6.047 cm. This data collection strategy has been shown to provide high resolution, large redundancy and appropriate completeness in data sets [49]. The X-ray data collection strategy at 100 K is shown in the Supplementary data. The number of frames collected was 7272, and integrated with SAINT [43] using a narrow frame integration method. Sorting, scaling, merging, and empirical correction for absorption of the set of intensities were performed with SORTAV [50]. The crystal structure of **1** was solved by direct methods using SIR92 and refined in the spherical atom approximation based on  $F^2$  using SHELXL97 included in the package WinGX. Molecular thermal ellipsoid plots and packing diagrams were generated using ORTEP32 [51] and CAMERON [52], respectively. All hydrogen atoms were located from the Fourier difference map and refined freely, along with an isotropic displacement parameter.

### 2.2. Multipole refinement

The aspherical atom refinement, based on  $F^2$ , was carried out using the XD package [53]. The module XDLSM, a full-matrix least-squares program, was used to carry out the multipolar refinement. Scattering factors for all atoms were derived from the Clementi and Roetti wave functions [54]. The total number of measured reflections was 15,286, and number of uniquely measured reflections was 2658. During the least-squares refinement, the function  $\sum w\{|F_o|^2 - K|F_c|^2\}^2$  was minimized in which out of 2658 reflections, 251 were eliminated owing to condition of  $l > 3\sigma(l)$  and hence 2407 reflections were included in the refinement. Initially only the scale factor was refined on all reflections in order to check the accuracy of the data transfer from SHELX to XD via XDINI. Then the scale factor was refined for all successive steps of the multipole refinement. In the next step, the positional coordinates and thermal parameters of all non-H-atoms were determined accurately by carrying out a higher order refinement,

using 1075 reflections with  $0.8 < \sin \theta/\lambda < 2.0 \text{ \AA}^{-1}$  and  $I > 3\sigma(I)$ . The space group being non-centrosymmetric, the origin was specified with respect to the coordinates of oxygen atom O1. In the following step, the positional coordinates and isotropic thermal parameters of the H-atoms were refined using the lower angle reflections ( $0.0 < \sin \theta/\lambda < 0.8 \text{ \AA}^{-1}$ ). Finally in the subsequent refinements, owing to unavailability of neutron scattering data, the positions of the methylene and hydroxyl hydrogen atoms were fixed at the average bond distance values obtained from reported neutron diffraction studies [55]. The multipole populations (up to hexadecapole for all non-H atoms) were then refined in a stepwise manner. For all H-atoms, the multipole expansion was truncated at  $l_{\text{max}} = 1$  (dipole, bond-directed) level. No restraints based on chemical symmetry were applied in the refinement of the multipole populations of the atoms; the molecular electroneutrality constraint was, however, switched on to ensure that the unit cell remained neutral throughout all refinements. In the next step, a single refinement of the  $\kappa$  parameters for all non-H-atoms was performed; a single  $\kappa'$  was then refined along with the respective  $\kappa$  parameter for each group of chemically distinct non-H-atoms until convergence was achieved. The  $\kappa$  and  $\kappa'$  values for all H atoms were fixed at 1.2. The data/parameter ratio on refinement of all variables is 13.83. Finally, all the multipole parameters (including the isotropic thermal parameters of H-atoms) were refined in order to obtain the final model of charge density distribution and these were checked for convergence. Modules XDFFT and XDFOUR were used to measure the residual electron density and the dynamic deformation density, respectively. In order to obtain a quantitative picture of the electronic structure, the module XDPROP was used for topological analysis of the electron densities. The presence of all critical points (whether bond or ring) were explored carefully. No intra-molecular (3, +1) ring critical points were observed, the existence of which might suggest the possibility of an intra-molecular O–H...O bond critical point.

### 2.3. Computational methods

Single-point energies and electron density distributions were calculated by generating a wave function based on the X-ray coordinates at the MPW1PW91/6-311+G (2d,p) level of theory, shown to perform well for diols and other larger hydrogen bonded systems at moderate computational cost [56]. The wave function was produced in pure Cartesians (6D 10F) with the options (scf = tight) and (int = ultrafine). All DFT calculations were performed using the GAUSSIAN03 suite of programs [57]. Input and output structures were visualised with GaussView [58]. Electron density contour maps were derived from the wave function using AIM2000 software [59], and any electrostatic multipole analysis carried out using MORPHY98 [60].

## 3. Results and discussion

The space group and unit cell dimensions for the crystalline ethane-1,2-diol, together with other essential experimental parameters and measures of goodness-of-fit, are shown in Table 1. The results are in agreement with those reported recently by Boese and co-workers [10f,10g]. The atom numbering nomenclature is shown in the ORTEP representation of ethane-1,2-diol in Fig. 1. Atomic fractional coordinates are given in Table 2. Geometric data for each ethane-1,2-diol unit are shown in Table 3. Electron density topological parameters for the intra-molecular bond critical points (BCPs) for all covalent bonds are given in Table 4 and that for the inter-molecular hydrogen bonds in Table 5. In addition, detailed data covering anisotropic displacement parameters, local coordinate axes, differences of mean-squares displacement amplitudes

**Table 1**

Experimental details at 100 K: Crystal data, structure solution and aspherical atom refinement of the unit cell containing four ethane-1,2-diol molecules.

Cell setting, space group	Orthorhombic, $P2_12_12_1$ *
<i>Unit cell dimensions</i>	
<i>a</i> (Å)	4.9993(3)
<i>b</i> (Å)	6.9031(4)
<i>c</i> (Å)	9.2499(5)
<i>V</i> (Å <sup>3</sup> )	319.05(3)
<i>Z</i>	4
$\rho_{\text{calcd}}$ (g/cm <sup>3</sup> )	1.29
$\mu$ (mm <sup>-1</sup> )	0.115
<i>F</i> (000)	136
$\theta$ Range (°), ( $\sin \theta/\lambda$ ) <sub>max</sub> (Å <sup>-1</sup> )	3.7–45.5, 1.00
Range of <i>h</i> , <i>k</i> , <i>l</i>	–10 → <i>h</i> → 9 –13 → <i>k</i> → 13 –18 → <i>l</i> → 18
Measured reflections	15,286
Unique reflections	2686
Observed reflections [ $I > 3\sigma(I)$ ]	2407
Overall completeness	100%
$R_{\text{int}}$	0.016
Refinement based on	$F^2$
$R(F)$ , $R_w(F)$	0.0267, 0.036
$R(F^2)$ , $R_w(F^2)$	0.0395, 0.061
Goodness of fit ( <i>S</i> )	2.1611
$N_{\text{obs}}/N_{\text{par}}$	13.83
Range of residual ED in asymmetric unit (e Å <sup>-3</sup> )	0.240/–0.181

\* The "absolute configuration" was not determined.

(DMSDA), multipole population coefficients and kappa values, population parameters for dipole, quadrupole, octupole and hexadecapole moments are given in the [Supplementary data](#).

The crystal structure of the ethane-1,2-diol with four molecules per unit cell is characterised by the diol being in the *g'Gt* (*g'Ga*) conformation. This conformation corresponds to the global minimum found both experimentally and theoretically for the monomer in

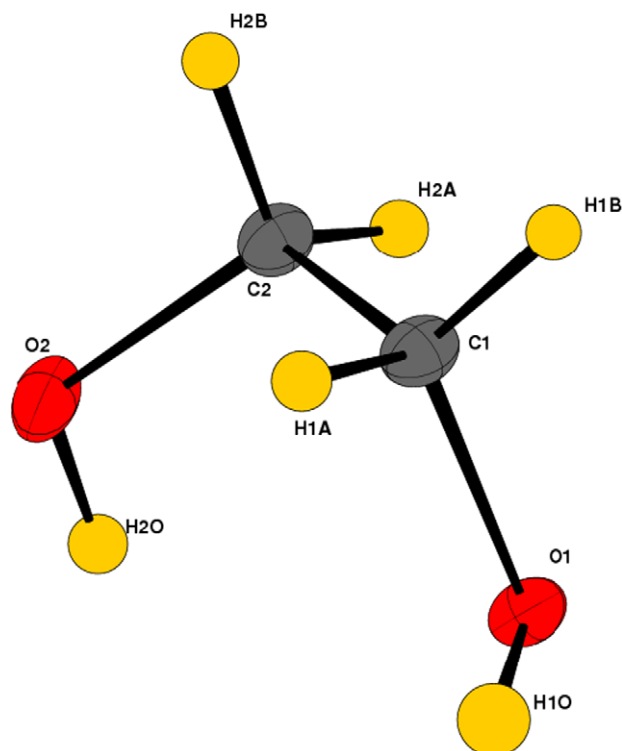


**Fig. 1.** An ORTEP view of ethane-1,2-diol, showing the atom numbering scheme. Displacement ellipsoids are drawn at 50% probability level and hydrogen atoms are shown as small spheres of arbitrary radii.

**Table 2**  
Atomic fractional coordinates of ethane-1,2-diol at 100 K after XD refinement.

Atom	X	Y	Z
O(1)	0.0049(2)	0.1443(1)	0.1130(1)
O(2)	0.2727(1)	0.0005(1)	−0.1429(1)
C(2)	−0.0102(1)	−0.0006(1)	−0.1230(3)
C(1)	−0.0867(1)	−0.0207(1)	0.0342(1)
H(1A)	0.0079	−0.1442	0.0875
H(2A)	−0.0971	0.1318	−0.1676
H(2B)	−0.0813	−0.1125	−0.1740
H(1B)	−0.2705	−0.0348	0.0412
H(2O)	0.3449	0.1277	−0.1248
H(1O)	0.0868	0.1022	0.2023

**Table 3**  
Bond lengths, bond angles and torsion angles (dihedrals) of ethane-1,2-diol, obtained after XD refinement at 100 K.

<i>(a) Bond lengths (Å)</i>	
O(1)–C(1)	1.4287(5)
O(2)–H(1O)	0.9670
O(2)–C(2)	1.4264(7)
O(2)–H(2O)	0.9670
C(2)–C(1)	1.5089(6)
C(2)–H(2A)	1.0920
C(2)–H(2B)	1.0920
C(1)–H(1A)	1.0920
C(1)–H(1B)	1.0920
<i>(b) Bond angles (°)</i>	
C(1)–O(1)–H(1°)	109.43(2)
C(2)–O(2)–H(2°)	110.53(5)
O(2)–C(2)–C(1)	112.07(4)
O(2)–C(2)–H(2 <sup>a</sup> )	110.06(4)
O(2)–C(2)–H(2B)	107.60(4)
C(1)–C(2)–H(2 <sup>a</sup> )	109.84(4)
C(1)–C(2)–H(2B)	107.54(4)
H(2A)–C(2)–H(2B)	109.66(4)
O(1)–C(1)–C(2)	109.71(4)
O(1)–C(1)–H(1 <sup>a</sup> )	104.68(4)
O(1)–C(1)–H(1B)	111.49(5)
C(2)–C(1)–H(1A)	113.36(4)
C(2)–C(1)–H(1B)	109.15(4)
H(1A)–C(1)–H(1B)	108.43(4)
<i>(c) Torsional angles (dihedrals) (°)</i>	
H(1O)–O(1)–C(1)–C(2)	−135.3(1)
H(1O)–O(1)–C(1)–H(1A)	−13.3(1)
H(1O)–O(1)–C(1)–H(1B)	103.7(1)
H(2O)–O(2)–C(2)–C(1)	−82.1(1)
H(2O)–O(2)–C(2)–H(2A)	40.5(1)
H(2O)–O(2)–C(2)–H(2B)	159.9(1)
O(2)–C(2)–C(1)–O(1)	64.1(1)
O(2)–C(2)–C(1)–H(1A)	−52.5(1)
O(2)–C(2)–C(1)–H(1B)	−173.5(1)
H(2A)–C(2)–C(1)–O(1)	−58.6(1)
H(2A)–C(2)–C(1)–H(1A)	−175.2(1)
H(2A)–C(2)–C(1)–H(1B)	63.9(1)
H(2B)–C(2)–C(1)–O(1)	−177.9(1)
H(2B)–C(2)–C(1)–H(1A)	65.5(1)
H(2B)–C(2)–C(1)–H(1B)	−55.4(1)

**Table 4**  
Topological features of the electron density at the intra-molecular bond critical points.

Bond	$\rho_b$ ( $e/\text{Å}^3$ )	$\nabla^2\rho_b$ ( $e/\text{Å}^5$ )	$R_{ij}$ (Å)	$\lambda_1$ ( $e/\text{Å}^5$ )	$\lambda_2$ ( $e/\text{Å}^5$ )	$\lambda_3$ ( $e/\text{Å}^5$ )
O(1)–C(1)	1.83(4)	−15.37(20)	1.4287	−16.06	−12.56	13.25
O(1)–H(1O)	2.24(7)	−30.60(52)	0.9670	−37.11	−35.05	41.56
O(2)–C(2)	1.82(4)	−13.91(17)	1.4264	−15.24	−12.83	14.16
O(2)–H(2O)	2.16(7)	−32.20(53)	0.9670	−37.20	−34.98	39.98
C(1)–C(2)	1.90(3)	−18.67(9)	1.5089	−16.25	−12.95	10.53
C(2)–H(2A)	1.89(7)	−20.19(22)	1.0930	−19.61	−16.19	15.62
C(2)–H(2B)	1.83(7)	−13.40(27)	1.0930	−17.92	−14.31	18.82
C(1)–H(1A)	1.76(6)	−13.99(18)	1.0930	−16.30	−14.42	16.73
C(1)–H(1B)	1.81(6)	−11.65(28)	1.0930	−19.14	−14.74	22.24

Definitions:  $\rho_b$ , electron density at the bond critical point;  $\nabla^2\rho_b$ , Laplacian at the bond critical point;  $R_{ij}$ , bond length;  $\lambda_1$ ,  $\lambda_2$ ,  $\lambda_3$ , principal components of  $\nabla^2\rho_b$ .

**Table 5**  
Topological and geometrical features for inter-molecular non-covalent interactions stabilising the crystal structure of ethane-1,2-diol. Units:  $\rho_b/e\text{Å}^{-3}$ ;  $R_{ij}$ , Å;  $\nabla^2\rho_b$ ,  $\lambda_1$ ,  $\lambda_2$ ,  $\lambda_3/e\text{Å}^{-5}$ . Definitions:  $\rho_b$ , electron density at the bond critical point;  $\nabla^2\rho_b$ , Laplacian at the bond critical point;  $R_{ij}$ , donor–acceptor distance, R1 and R2 are the distances of the acceptor and donor atom from the BCP.

Interaction	$R_{ij}$ (Å)	$\rho(r)$ ( $e/\text{Å}^3$ )	$\nabla^2\rho(r)$ ( $e/\text{Å}^5$ )	R1 (Å)	R2 (Å)
O–H...O					
O(1)...X3_H(2O) <sup>1</sup>	1.7689	0.22(2)	3.311(20)	1.1685	0.6004
O(2)...X2_H(1O)	1.7474	0.24(2)	3.878(16)	1.1607	0.5867
C–H...O					
O(1)...X2_H(2B)	2.9030	0.028(4)	0.406(1)	1.6430	1.2599
O(2)...X2_H(1A)	2.9165	0.022(3)	0.343(3)	1.6713	1.2453
O(2)...X3_H(1A)	2.7908	0.024(4)	0.404(3)	1.6343	1.1566
C–H...H–X					
H(2A)...X4_H(2B)	2.4851	0.022(4)	0.366(2)	1.1881	1.2970
H(2A)...X3_H(1O)	2.4903	0.021(2)	0.258(2)	1.1867	1.3036

<sup>1</sup> The abbreviation O(1)...X3\_H(2O) means that the O1 and H<sub>2</sub>O, attached to O2, belonging to two ethane-diol units are linked by a (3, −1) bond critical point (BCP) where X3 refers to the symmetry code relating the two diol units: X1 = +X, +Y, +Z; X2 = ½ − X, −Y, ½ + Z; X3 = ½ + X, ½ − Y, −Z. X4 = −X, ½ + Y, ½ − Z.

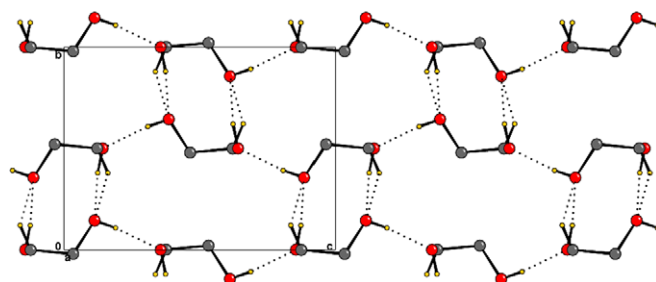


**Fig. 2.** Packing view of the compound forming O–H...O, C–H...O hydrogen bonds generating a sheet-like structure down the *bc*-plane.

the gas-phase [5–7]. The torsion (dihedral) angles for ethane-1,2-diol in the crystal are as follows, with the gas-phase results [22] shown in parentheses: H–O–C–C = −82.1(1)°/(−50.8°); O–C–C–O = +64.1(1)°/(+60.9°); C–C–O–H = −135.3(1)°/(−164.7°). The crystal is stabilised by a complex three-dimensional network of inter-molecular hydrogen bonds, both O–H...O and C–H...O, not only along lines ('*c*'-axis – O–H...O (short)) of head-to-tail ethane-1,2-diol molecules but also between rows ('*c*' crystal axis – O–H...O (long)) and columns ('*b*' crystal axis – C–H...O), forming a zigzag network. This is not immediately apparent in Fig. 2 because of overlapping atoms orthogonal to the plane of the figure. It has been suggested by Desiraju and Steiner that C–H...O hydrogen bonding may play a significant role in stabilising crystal structure, based on close-contact data obtained from crystallographic databases [61]. The C–H...O interaction clearly plays a role in stabilising the ethane-1,2-diol crystal structure. It is noteworthy that previous

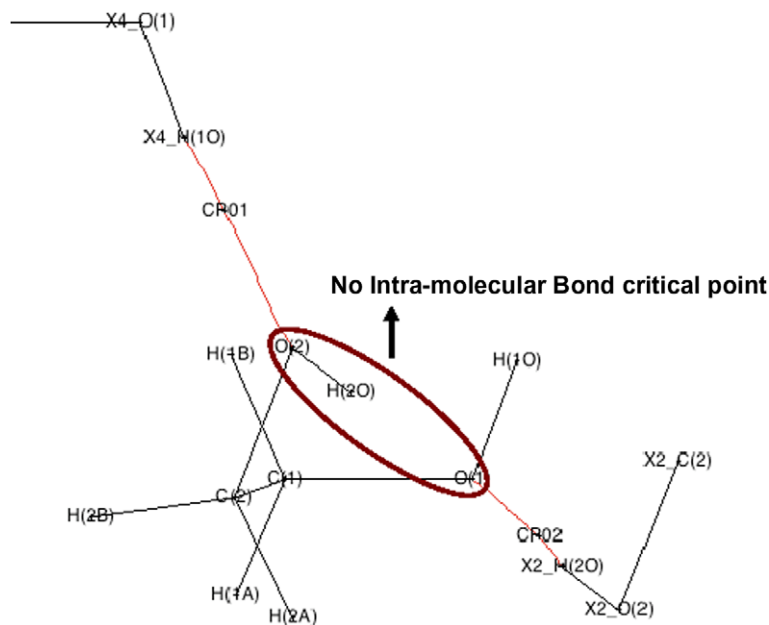


**Fig. 3.** Experimental intra- and inter-molecular bond paths as observed in ethane-1,2-diol. Red lines indicate inter-molecular bond paths and CP01 and CP02 depict the bond critical points for two O–H...O inter-molecular hydrogen bonds. (For interpretation of the references to color in this figure legend, the reader is referred to the web version of this paper.)

crystallographic studies [10f,10g] have not recognized the importance of C–H...O interactions in ethane-1,2-diol.

Fig. 3 depicts the intra- and inter-molecular O–H...O bond paths as observed in ethane-1,2-diol which clearly indicate that there is no evidence for the presence of a (3, –1) bond critical point (BCP) for a putative intra-molecular O–H...O interaction. This is further corroborated with calculated electron density maps of the ethane-1,2-diol molecule in the crystal (Figs. 4 and 5) which indicate absence of intra-molecular H-bonding. This is also in total agreement with previous *ab initio* and DFT theoretical studies of ethane-1,2-diol in the gas-phase [3,22–27] and points to there being no experimental electron density evidence for an intra-molecular hydrogen bond.

The finding that the crystal structure for ethane-1,2-diol preserves the *gauche* configuration in the crystalline state in the ab-

sence of any direct experimental evidence for intra-molecular hydrogen bonding raises the important question; what is the driving force that maintains this configuration if it is not primarily the O–H...O interaction as frequently assumed in the literature? As has been pointed out by a number of authors [3,17,22–27], hyper-conjugative effects such as  $n_o \Rightarrow [C-H]^*$  and  $[C-H] \Rightarrow [O-H]^*$  in the 2-substituted ethanols are energetically more significant than the  $n_o \Rightarrow [O-H]^*$  interaction except in planar or quasi-planar transition states [62] by a few kcal/mol. It has been pointed out by one of us [3] that vicinal diols from a wide range of molecular systems show

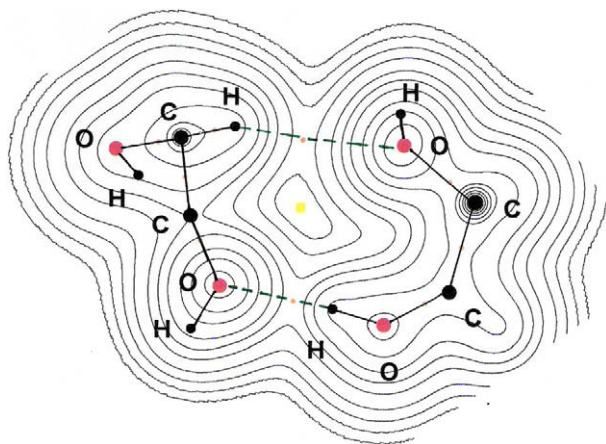


**Fig. 4.** Theoretical charge density contour map at the MPW1PW91/6–311++G(2d,p) level of theory obtained from coordinates of a unit cell, showing the C–H...O and one of the O–H...O interactions (the corresponding BCP's are depicted by orange opaque circle) surrounding a (3, +1) RCP (opaque yellow circle). (For interpretation of the references to color in this figure legend, the reader is referred to the web version of this paper.)

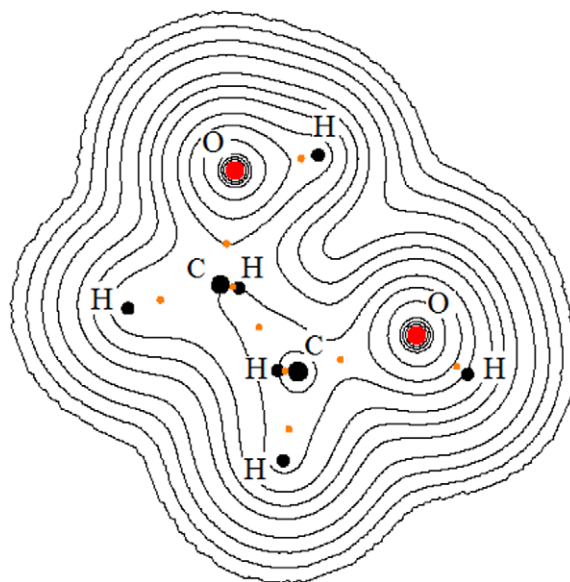


**Fig. 5.** Theoretical electron density map for an ethane-1,2-diol sub-unit obtained at the MPW1PW91/6–311++G(2d,p) level showing the lack of a (3, –1) BCP and thus of an intra-molecular hydrogen bond for the O–H/O–H interaction. The opaque orange circles depict intra-molecular bond critical points (BCP's) for ethane-1,2-diol. (For interpretation of the references to color in this figure legend, the reader is referred to the web version of this paper.)

a remarkably sharp donor–acceptor distance cut-off around 2.08–2.10 Å, apparently corresponding to the point at which the overlap integral for the occupied–unoccupied orbitals (hyperconjugation) exceeds that for the occupied–occupied orbitals (steric repulsion). In both the crystal structure and the gas-phase monomer the oxygen–hydrogen spacing is far in excess of this cut-off value, 2.7677 Å and 2.3379 Å, respectively. Though the distance in the gas-phase is less than the sum of *van der Waals* radii of O and H (2.6 Å), it is more than the sum of ‘hydrogen bond radii’ (2.0 Å), appropriate for OH (0.7 Å) and O (1.3 Å), as proposed by Raghavendra et al. recently [35]. Clearly, summation of the classical *van der Waals* atomic radii is not suitable as a criterion for determining whether or not there is hydrogen bonding. This procedure gives cut-off values that are generally much too high except perhaps for very weak dispersive interactions and should, therefore, not be used [31–35]. Observation of small red-shift in vibrational frequencies, again, is clearly not sufficient to conclude the presence of intra-molecular hydrogen bonding, in the absence of NMR spectroscopic evidence [17] and the absence of a BCP from both theoretical [3,22–26] and experimental electron density studies, reported here.

#### 4. Conclusions

*In situ* cryocrystallization experiments followed by careful charge density analysis indicate that ethane-1,2-diol preserves the *gauche* conformation in the crystalline state, as has been established previously [10]. This occurs, however, in the clear absence of an intra-molecular hydrogen bond [no (3, –1) BCP], even though a donor–acceptor distance of 2.77 Å and an O–H...O angle,  $\theta = 90.1^\circ$  between the hydrogen donor H<sub>2</sub>O and acceptor O1 exists in the geometry. Moreover, no (3, +1) RCP was found in this region. It thus seems likely that the driving force maintaining this conformation in the absence of intra-molecular hydrogen bonding is generated by hyper-conjugative effects between the C–H and O–H bonds, as previously suggested [3]. Overall crystal structure is stabilised by inter-molecular hydrogen bonds involving O–H...O and C–H...O interactions.

The results presented here are from crystal structure and cannot rule out the presence of an intra-molecular hydrogen bond in an isolated molecule. However, as ethane-1,2-diol is used as part of the training set for parametrization of molecular mechanics programs, which will eventually be used for modeling condensed phase, the results presented here should be given due consideration.

#### Acknowledgements

We thank the Department of Science and Technology, India for data collection on the CCD facility under the IRHPA-DST program. Deepak Chopra thanks Vijay Thiruvengadam for his constant presence during the experiments, CSIR and IISc for a research fellowship. R.A.K. acknowledge financial support from the Deutsche Forschungsgemeinschaft as part of a program Grant (DFG SFB284/A1) during the early stages of this work, as well as continuing support from the Neumann Institute for Computing (NIC) Forschungszentrum Jülich in the form of computational facilities on the IBM JUMP supercomputer. E.A. thanks IUPAC for supporting the formation of a task group to define hydrogen bonds, which motivated the discussions with R.A.K. and T.N.G., leading to this work.

#### Appendix A. Supplementary data

Anisotropic displacement parameters, local coordinate axes, differences of mean-squares displacement amplitudes (DMSDA), multipole population coefficients and kappa values, population

parameters for dipole, quadrupole, octupole and hexadecapole moments, Laplacian and deformation density maps are given in the Supplementary data. Supplementary data associated with this article can be found, in the online version, at [doi:10.1016/j.molstruc.2009.11.021](https://doi.org/10.1016/j.molstruc.2009.11.021).

#### References

- [1] G. Frenking, A. Krapp, *J. Comput. Chem.* 28 (2007) 15–24.
- [2] E.L. Eliel, “Stereochemistry of Carbon Compounds” McGraw-Hill, New York, 1962, p. 131: “...ethylene glycol may exist in two distinct stable conformations..., the anti conformation and gauche conformation (of which there are two enantiomers). Only in the latter are the hydroxyl groups close enough together to give rise to an intra-molecular bond...”.
- [3] R.A. Klein, *Chem. Phys. Lett.* 429 (2006) 633–637.
- [4] A.J. Lopes Jesus, M.T.S. Rosado, I. Reva, R. Fausto, M. Emrinda Eusebio, J.S. Redinha, *J. Phys. Chem. A* 110 (2006) 4169–4179.
- [5] O. Bastiansen, *Acta Chem. Scand.* 3 (1949) 415–421.
- [6] P. Buckley, P.A. Giguère, *Can. J. Chem.* 45 (1967) 397–407.
- [7] K.-M. Marstokk, H. Møllendal, *J. Mol. Struct. (Theochem)* 22 (1974) 301–303.
- [8] D. Christen, L.H. Coubert, R.D. Suenram, F.J. Lovas, *J. Mol. Spectrosc.* 172 (1995) 57–77.
- [9] D. Christen, L.H. Coudert, J.A. Larsson, D. Cremer, *J. Mol. Spectrosc.* 205 (2001) 185–196.
- [10] (a) A. Manisse-Morgant, J.L. Beaudoin, A. Bechneane, M. Harnad, *C.R. Acad. Sci. B* 273 (1971) 293–296; (b) M. Espanol, A. Manisse, J.L. Beaudoin, M. Harnad, *C.R. Acad. Sci. C* 281 (1975) 445–448; (c) A. Manisse, J.L. Beaudoin, M. Espanol, M. Harnad, *C.R. Acad. Sci. B* 281 (1975) 243–246; (d) I. Bako, T. Grosz, G. Palinkas, M.C. Bellissent-Funel, *J. Chem. Phys.* 118 (2003) 3215–3221; (e) C.P. Brock, *Acta Crystallogr. Sect. B* 58 (2002) 1025–1031; (f) R. Boese, H.-C. Weiss, *Acta Crystallogr. Sect. C* 54 (1998) IUC9800024; (g) V.R. Thalladi, R. Boese, H.-C. Weiss, *Angew. Chem. Int. Ed.* 39 (2000) 918–922.
- [11] B. Renault, E. Cloutet, H. Cramail, T. Tassaing, M. Besnard, *J. Phys. Chem. A* 111 (2007) 4181–4187.
- [12] (a) D.L. Howard, P. Jørgensen, H.G. Kjaergaard, *J. Am. Chem. Soc.* 127 (2005) 17096–17103; (b) D.L. Howard, H.G. Kjaergaard, *J. Phys. Chem. A* 110 (2006) 10245–10250.
- [13] (a) L.P. Kuhn, *J. Am. Chem. Soc.* 74 (1952) 2492–2499; (b) *J. Am. Chem. Soc.* 76 (1954) 4323–4326; (c) *J. Am. Chem. Soc.* 80 (1958) 5950–5954; (d) M. Kuhn, W. Lüttke, R. Mecke, *Z. Anal. Chem.* 170 (1959) 106–114.
- [14] L.J. Bellamy, *The Infrared Spectra of Complex Molecules*, third ed., vol. 1, Chapman & Hall, London, 1975.
- [15] C.M. Pearce, J.K.M. Sanders, *J. Chem. Soc. Perkin Trans. 1* (1994) 1119–1124.
- [16] R.L. Thurlkill, G.R. Grimsley, J.M. Scholtz, C.N. Pace, *J. Mol. Biol.* 362 (2006) 594–604.
- [17] K.A. Petterson, R.S. Stein, M.D. Drake, J.D. Roberts, *Magn. Reson. Chem.* 43 (2005) 225–230.
- [18] S.O. Jonsdottir, R.A. Klein, *Fluid Phase Equilib.* 132 (1997) 117–127.
- [19] S.O. Jonsdottir, W.J. Welsh, K. Rasmussen, R.A. Klein, *New J. Chem.* (1999) 153–163.
- [20] (a) K.-M. Marstokk, H. Møllendal, *J. Mol. Spectrosc.* 22 (1974) 301–303; (b) D. Christen, H.S.P. Mueller, *Phys. Chem. Chem. Phys.* 5 (2003) 3600–3605 (and references cited therein).
- [21] (a) P. Bultinck, A. Goeminne, D. Van der Vondel, *J. Mol. Struct. (Theochem)* 334 (1995) 101–107. *J. Mol. Struct.* 357 (1995) 19–32; (b) A.J. Lopes-Jesus, M.T. Rosada, M.L.P. Leita, J.S. Redinha, *J. Phys. Chem. A* 107 (2003) 3891–3897.
- [22] (a) R.F.W. Bader, *Atoms in Molecules: A Quantum Theory*, Oxford University Press, Oxford, 1990; (b) R.F.W. Bader, *J. Phys. Chem. A* 102 (1998) 7314–7323; (c) R.A. Klein, *J. Comput. Chem.* 23 (2002) 585–599.
- [23] R.A. Klein, *J. Comput. Chem.* 24 (2003) 1120–1131.
- [24] C. Trindle, P. Crum, K. Douglass, *J. Phys. Chem. A* 107 (2003) 6236–6242.
- [25] M. Mandado, A.M. Grana, R.A. Mosquera, *Phys. Chem. Chem. Phys.* 6 (2004) 4391–4396.
- [26] M.M. Deshmukh, N.V. Sastry, S.R. Gadre, *J. Chem. Phys.* 121 (2004) 12402–12410.
- [27] D.L. Crittenden, K.C. Thompson, M.J.T. Jordan, *J. Phys. Chem. A* 109 (2005) 2971–2977.
- [28] U. Koch, P.L.A. Popelier, *J. Phys. Chem.* 99 (1995) 9747–9754.
- [29] L.F. Pacios, P.C. Gómez, *J. Comput. Chem.* 22 (2001) 702–716.
- [30] (a) A. Volkov, C. Gatti, Y. Abramov, P. Coppens, *Acta Crystallogr. Sect. A* 56 (2000) 252–258; (b) Y. Abramov, A. Volkov, G. Wu, P. Coppens, *Acta Crystallogr. Sect. A* 56 (2000) 585–591; (c) T. Koritsanzky, P. Coppens, *Chem. Rev.* 101 (2001) 1583–1621; (d) A. Volkov, P. Coppens, *Acta Crystallogr. Sect. A* 57 (2001) 395–405.
- [31] R.A. Klein, *Chem. Phys. Lett.* 425 (2006) 128–133.
- [32] P.K. Mandal, E. Arunan, *J. Chem. Phys.* 114 (2001) 3880–3882.

- [33] M. Goswami, P.K. Mandal, D.J. Ramdass, E. Arunan, *Chem. Phys. Lett.* 393 (2004) 22–27.
- [34] B. Lakshmi, A.G. Samuelson, K.V. Jovan Jose, S.R. Gadre, E. Arunan, *New J. Chem.* 29 (2005) 371–377.
- [35] B. Raghavendra, P.K. Mandal, E. Arunan, *Phys. Chem. Chem. Phys.* 8 (2006) 5276–5286.
- [36] R.A. Klein, *Chem. Phys. Lett.* 433 (2006) 165–169.
- [37] S. Mendonca, G.P. Johnson, A.D. French, R.A. Laine, *J. Phys. Chem. A* 106 (2002) 4115–4124.
- [38] P.L.A. Popelier, *Atoms in Molecules: An Introduction*, Pearson Education, London, 2000.
- [39] C. Manca, C. Tanner, S. Leutwyler, *Int. Rev. Phys. Chem.* 24 (2005) 457–488.
- [40] Y.-L. Li, X.-L. Sun, Y.-L. Wu, *Tetrahedron* 50 (1994) 10727–10738.
- [41] R.N. Patel, A. Banerjee, Y.R. Pendri, J. Liang, C.-P. Chen, R. Mueller, *Tetrahedron: Asymmetry* 17 (2006) 175–178.
- [42] X. Wang, L. Wang, H. Li, X. Tang, F.-C. Chang, *J. Appl. Polym. Sci.* 77 (2000) 184–188.
- [43] Bruker SMART (Version 6.028), SAINT (Version 6.02), XPREP. Bruker AXS Inc., Madison, WI, USA, 1998.
- [44] G.M. Sheldrick, SADABS, University of Göttingen, Göttingen, Germany, 1996.
- [45] A. Altomare, G. Cascarano, C. Giacovazzo, A. Guagliardi, M.C. Burla, G. Polidori, M. Camalli, *J. Appl. Crystallogr.* 27 (1994) 435–436.
- [46] G.M. Sheldrick, SHELXS97 and SHELXL97, University of Göttingen, Göttingen, Germany, 1997.
- [47] M. Nardelli, *J. Appl. Crystallogr.* 28 (1995) 659.
- [48] A.L. Spek, *J. Appl. Crystallogr.* 36 (2003) 7–13.
- [49] (a) P. Munshi, T.N. Guru Row, *Acta Crystallogr. Sect. B* 58 (2002) 1011–1017; (b) P. Munshi, T.N. Guru Row, *Acta Crystallogr. Sect. B* 59 (2003) 159.
- [50] (a) R.H. Blessing, *Crystallogr. Rev.* 1 (1987) 3–58; (b) R.H. Blessing, *J. Appl. Crystallogr.* 22 (1989) 396–397; (c) R.H. Blessing, *Acta Crystallogr. Sect. A* 51 (1995) 33–38.
- [51] L.J. Farrugia, *J. Appl. Crystallogr.* 30 (1997) 568.
- [52] D.M. Watkin, L. Pearce, C.K. Prout, CAMERON – A Molecular Graphics Package, Chemical Crystallography Laboratory, University of Oxford, Oxford, 1993.
- [53] T. Koritsanszky, T. Richter, P. Macci, C. Gatti, S. Howard, P.R. Mallinson, L. Farrugia, Z.W. Su, N.K. Hansen, XD: A Computer Program Package for Multipole Refinement and Analysis of Electron Densities from Diffraction Data, Technical 521 Report, Freie University of Berlin, Berlin, Germany, 2003.
- [54] E. Clementi, C. Roetti, *Atomic Data and Nuclear Data Tables* 14 (1974) 177.
- [55] F.H. Allen, O. Kennard, D.G. Watson, L. Brammer, A.G. Orpen, R. Taylor, *J. Chem. Soc. Perkin Trans. 2* (1987) S1–S19.
- [56] R.A. Klein, B. Mennucci, J. Tomasi, *J. Phys. Chem. A* 108 (2004) 5851–5863.
- [57] M.J. Frisch, G.W. Trucks, H.B. Schlegel, G.E. Scuseria, M.A. Robb, J.R. Cheeseman, V.G. Zakrzewski, J.A. Montgomery Jr, R.E. Stratmann, J.C. Burant, S. Dapprich, J.M. Millam, A.D. Daniels, K.N. Kudin, M.C. Strain, O. Farkas, J. Tomasi, V. Barone, M. Cossi, R. Cammi, B. Mennucci, C. Pomelli, C. Adamo, S. Clifford, J. Ochterski, G.A. Petersson, P.Y. Ayala, Q. Cui, K. Morokuma, N. Rega, P. Salvador, J.J. Dannenberg, D.K. Malick, A.D. Rabuck, K. Raghavachari, J.B. Foresman, J. Cioslowski, J.V. Ortiz, A.G. Baboul, B.B. Stefanov, G. Liu, A. Liashenko, P. Piskorz, I. Komaromi, R. Gomperts, R.L. Martin, D.J. Fox, T. Keith, M.A. Al-Laham, C.Y. Peng, A. Nanayakkara, M. Challacombe, P.M.W. Gill, B. Johnson, W. Chen, M.W. Wong, J. L. Andres, C. Gonzalez, M. Head-Gordon, E.S. Replogle, J.A. Pople, *Gaussian-98, Revision A.11.3*, Gaussian, Inc., Wallingford, CT, 2002.
- [58] T. Keith, J. Millam, K. Eppinnett, W.L. Hovell, R. Gilliland, GaussView, Version 3.09, Dennington II, Roy, Semichem, Inc., Shawnee Mission, KS, 2003.
- [59] (a) F.H. Biegler-König, *J. Comput. Chem.* 21 (2000) 1040–1048; (b) F.H. Biegler-König, J. Schönbohm, D. Bayles, *J. Comput. Chem.* 22 (2001) 545–559; (c) F.W. Biegler-König, R.W.F. Bader, T.H. Tang, *J. Comput. Chem.* 3 (1982) 317–328.
- [60] MORPHY98: a topological analysis program written by P.L.A. Popelier with a contribution from R.G.A. Bone (UMIST, Manchester, England); P.L.A. Popelier, *Comput. Phys. Commun.* 93 (1996) 212–240; P.L.A. Popelier, *Theor. Chim. Acta* 87 (1994) 465–476; P.L.A. Popelier, *Mol. Phys.* 87 (1996) 1169–1187; P.L.A. Popelier, *Comput. Phys. Commun.* 108 (1998) 180–190; P.L.A. Popelier, *Can. J. Chem.* 74 (1996) 829–838.
- [61] G.R. Desiraju, T. Steiner, *The Weak Hydrogen Bond*, Oxford University Press, Oxford, 1999.
- [62] R.A. Klein, Unpublished results, 2009.